Journal of Nuclear Materials 384 (2009) 77–80

Contents lists available at ScienceDirect

Journal of Nuclear Materials

journal homepage: www.elsevier.com/locate/jnucmat

Letter to the Editor

The role of Fe on the solubility of Nb in α-Zr

O.T. Woo *, M. Griffiths

AECL Chalk River Laboratories, Deformation Technology Branch, Chalk River, Ontario, Canada K0J 1J0

ARTICLE INFO

Article history:
Received 18 March 2008
Accepted 19 October 2008

ABSTRACT

The solid solubility of Nb in α-Zr is an important parameter that has a potential impact on the corrosion properties of Zr–Nb alloys at reactor operating temperatures, i.e. below the monotectoid temperature. Work on dilute Zr–Nb alloys has shown that Fe is a common impurity that confounds the assessment of the solid solubility limit for Nb in Zr. This is because Fe has a very low solubility limit and it forms precipitates with both Nb and Zr. To assess the effect of Fe on the phases formed in the binary Zr–Nb alloy system, alloys containing 0.1–0.7 wt% Nb and <11 to 470 wt ppm Fe were heat-treated at temperatures between 575 °C and 600 °C and examined by transmission electron microscopy. Results indicate that, even at a concentration ⩽ 24 ppm, Fe readily combines with Nb to form precipitates in the alloys with Nb contents in the range of 0.20–0.29 wt%. However, β-Nb particles were not observed for these same alloys and were only seen when the Nb content was ⩾ 0.49 wt%. Because β-Nb particles were not found in the 0.29 wt% Nb alloy and the precipitation was estimated to have a negligible effect on the amount of Nb remaining in solution (reduced by <0.001 wt%), it is proposed that the solubility limit of Nb in a true binary Zr–Nb alloy would be between 0.29 and 0.49 wt%.

1. Introduction

Zr–2.5wt%Nb alloys are used for pressure tubing in CANDU[1] nuclear reactors. The tubes are extruded at 815 °C, cold worked 27%, and stress relieved at 400 °C for 24 h, resulting in a structure consisting of elongated grains of hexagonal-close-packed (hcp) α-Zr, mostly surrounded by a thin network of filaments of body-centred-cubic β-Zr. These β-Zr filaments are metastable and initially contain about 20% Nb. The stress-relief treatment results in partial decomposition of the β-Zr filaments with the formation of hexagonal-close-packed ω-phase particles that are low in Nb, surrounded by an Nb-enriched β-Zr matrix.

The corrosion behaviour of Zr–2.5wt%Nb is sensitive to its metallurgical microstructure [1]. The post-irradiation corrosion resistance of Zr–2.5Nb improves with extended exposure to irradiation [1–4]. The improved corrosion resistance has been attributed to the radiation-enhanced precipitation of β-Nb particles and the concomitant reduction of the Nb concentration in the α-Zr during irradiation [3,4]. These results are consistent with work on dilute Zr–*x*Nb alloys ($x \leqslant 0.6$ wt%) [5] showing that the corrosion resistance improves when the Nb concentration is very close to the equilibrium solubility limit at the test temperature. Thus the solubility limit of Nb in α-Zr is of technological interest.

The room temperature solubility of Nb in α-Zr has been reported as 0.2 wt% [6], 0.8 wt% [7], and 1.1 wt% [6] for Zr–Nb alloys with the major impurities, oxygen and iron, ranging from 1230 to 1400 wt ppm and 550 to 900 wt ppm, respectively. Oxygen stabilizes the α-phase and iron stabilizes the β-phase. As niobium is also a β-stabilizer the Fe tends to segregate with Nb and form separate phases even at very low Fe and Nb concentrations. As it is very difficult to obtain Zr without some Fe being present as an impurity the Zr–Nb binary alloy systems is, in effect, a ternary system with Fe being the third element. As a result it is very difficult to determine the true solubility limit of Nb in the α-phase of a binary Zr–Nb alloy. This paper addresses the influence of Fe on the apparent solubility limit of Nb in α-Zr. In this work, the absence of particles containing Nb is used as an indication that all the Nb is in solid solution.

2. Experimental

Drop-cast Zr–Nb alloys with varying Nb and Fe concentrations were obtained from Teledyne Wah Chang for this work. Table 1 lists the materials together with their Nb, Fe and O contents. While the Fe contents of the alloys range from <50 (low) and 400 to 500 wt ppm (high), the O contents are not significantly different, varying from 880 to 1080 wt ppm. Compositions were chosen so that some samples had similar amounts of Nb and variable amounts of Fe. Other compositions were chosen having varying amounts of Nb (0.1–0.86 wt%) whilst maintaining the Fe content as low as possible (<50 wt ppm).

* Corresponding author. Tel.: +1 613 584 8811x44652; fax: +1 613 584 8214.
E-mail address: wooo@aecl.ca (O.T. Woo).

[1] CANada Deuterium Uranium, registered trademark of Atomic Energy of Canada Limited.

0022-3115/$ - see front matter © 2008 Elsevier B.V. All rights reserved.
doi:10.1016/j.jnucmat.2008.10.004

Table 1
Low Nb Zr alloys.

Alloy	Nb (wt%)	Fe (wt ppm)	O (wt ppm)	Heat treatment			Observed particles			
				600 °C (h)	580 °C (h)	575 °C (h)	Zr/Fe	Zr/Si (Fe, Ni, Cu)	Zr/Nb/Fe(Cr,Ni)[a]	β-Nb[b]
1	0.10 ± 0.01	<13	960	24		450	X	X		
2	0.20 ± 0.02	24 ± 7	930	24	96	450	X	X	X	
3	0.29 ± 0.03	<11	880	24	96	450		X	X	
4	0.49 ± 0.05	<11	910	24	96	350			X	X
5	0.69 ± 0.07	32 ± 9	900	24	96	350			X	X
6	0.86 ± 0.09	<11	770	24		99			X	X
7	0.30 ± 0.03	430 ± 40	1070	24	96				X	
8	0.70 ± 0.07	470 ± 50	1080	24		99			X	X

[a] Zr/Nb/Fe(Cr, Ni): Analyzed by electron micro-diffraction as a hexagonal phase, with a = 0.54 nm, and c = 0.88 nm. These particles contain varying trace amounts of Ni and/or Cr. Some of them also contain small amounts of Si and/or W present as impurities in the alloys.
[b] β-Nb: Analyzed by electron micro-diffraction as a bcc phase with a lattice parameter of =0.33 nm, corresponding to about 88–90 wt%Nb. Note the absence of Fe in this phase.

All alloys were initially given a heat treatment of 600 °C for 24 h both to homogenise the material and form the equilibrium phase close to the monotectoid temperature of the Zr–Nb binary system. Subsequent heat treatments were carried out below the monotectoid temperature, at 580 °C and 575 °C, to ensure that there was sufficient time at temperature to allow for the growth of precipitates that may nucleate at a temperature where the equilibrium β-Nb exists, [6], and improve the chances of their being observed by transmission electron microscopy (TEM). TEM specimens were prepared by punching 3-mm-diameter discs from 0.1-mm-thick slices that were cut from the annealed samples. Foils were then made by electropolishing with a solution of 10% perchloric acid in methanol at about −40 °C at a current density of about 0.01 A mm^{-2} using a Materials Science Northwest twin-jet apparatus. Transmission electron microscopy was performed using a Philips CM 30 electron microscope operating at 300 kV and equipped with an atmospheric thin window energy dispersive X-ray detector. The chemical composition of second phase precipitates was obtained by energy dispersive X-ray (EDX) analysis.

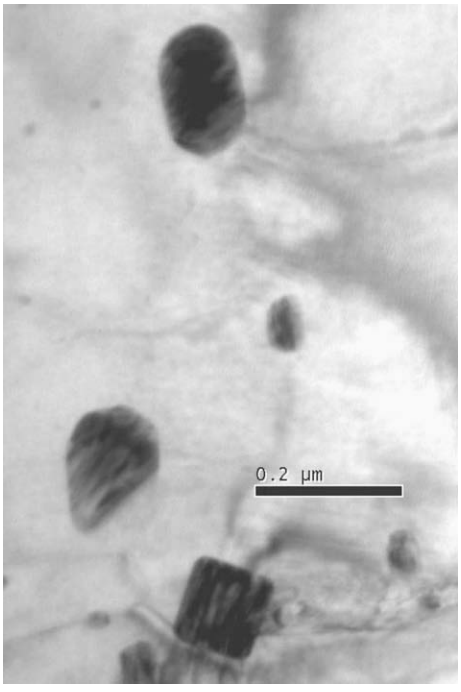

Fig. 1(a). TEM micrograph showing three 0.1 μm diameter particles in alloy #8 with 0.7 wt%Nb and 470 wt ppm Fe that was annealed at 580 °C for 99 h.

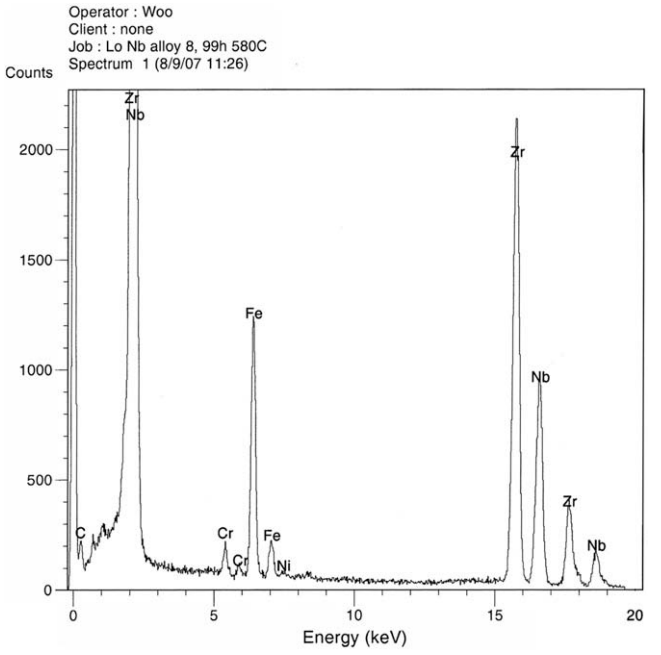

Fig. 1(b). Typical EDX spectrum of a 0.1 μm diameter particle shown in Fig. 1(a), showing the presence of Zr, Nb, Fe and traces of Ni in the particle. The C is from the contamination spot on the foil caused by the electron beam for analysis.

3. Observed particles

Four types of second phase particles were found in the alloys: Zr/Fe, Zr/Nb/Fe(Cr, Ni), β-Nb and Zr/Si(Fe, Ni, Cu) under various conditions. The observations are summarized in Table 1. Zr/Nb/Fe(Cr, Ni) particles that were up to 0.1 μm in diameter were readily observed in the high Fe and high Nb alloys (#7 and #8). Fig. 1(a) shows several particles in alloy #8 (0.7 wt%Nb, 470 wt ppm Fe) annealed at 580 °C for 99 h. A typical EDX spectrum from one such particle, Fig. 1(b), reveals the presence of Zr, Nb, Fe, and Cr with trace amounts of Ni. Electron micro-diffraction analysis of the larger particles in alloy #8 indicated that these particles had a hexagonal phase with lattice parameters of a = 0.54 nm and c = 0.88 nm, in agreement with published data [9,10]. β-Nb precipitates were observed as elongated particles in alloys having Nb concentrations $\geqslant$0.49 wt% (alloys #4, 5, 6 and 8). They were present at grain boundaries and in the grain interior, Fig. 2(a), and on subgrain boundaries, Fig. 2(b). In contrast to other precipitates observed in these alloys, the β-Nb precipitates do not contain Fe, see Fig. 2(c). Electron micro-diffraction analysis of the β-Nb precipitates was

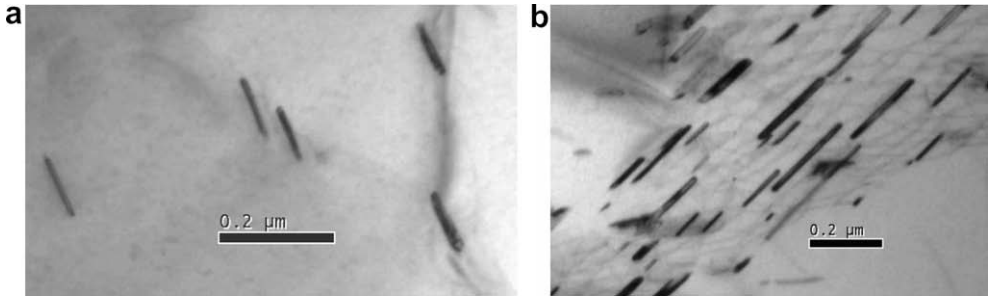

Fig. 2(a) and (b). Elongated β-Nb particles observed in an alloy having a Nb content ⩾0.49 wt%. They were seen in the grain interior and at grain boundaries in (a) and aligned on subgrain boundaries in (b). TEM foil is from alloy #5 that has 0.69 wt%Nb and 32 wt ppm Fe after annealing at 575 °C for 350 h.

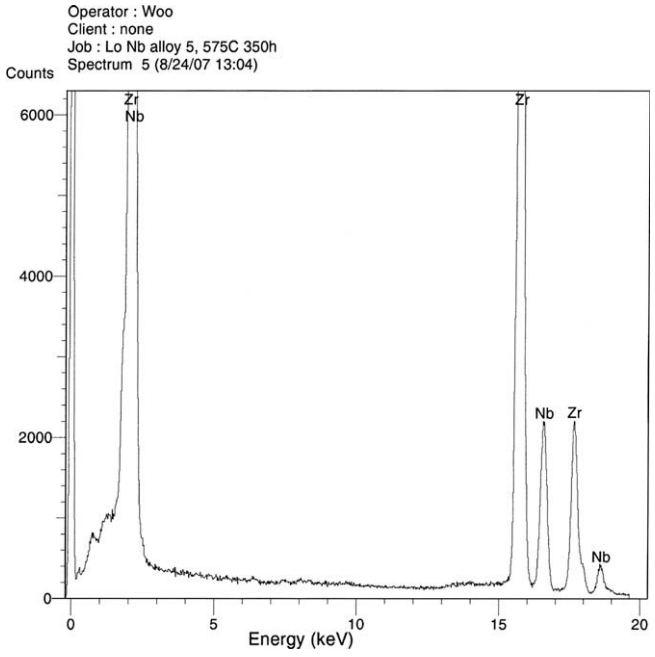

Fig. 2(c). EDX spectrum of a β-Nb particle showing the presence of Zr and Nb, with no Fe in the particle. Subsequent electron diffraction analysis shows a body-centred-cubic crystal structure with $a = 0.33$ nm, consistent with a Nb concentration of about 88 wt%Nb.

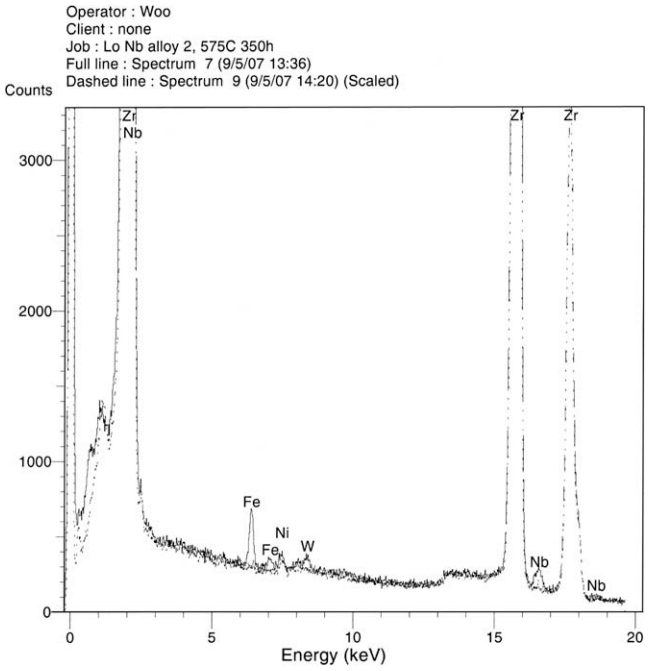

Fig. 3(b). EDX spectrum of a Zr/Nb/Fe particle in alloy #2 (0.2 wt%Nb and 24 wt ppm Fe) annealed at 575 °C for 350 h. The spectrum of the matrix is also included for comparison. Particle has traces of Ni and W. Top trace (solid line) is from the particle, while the bottom trace (dashed line) is from the α-Zr matrix.

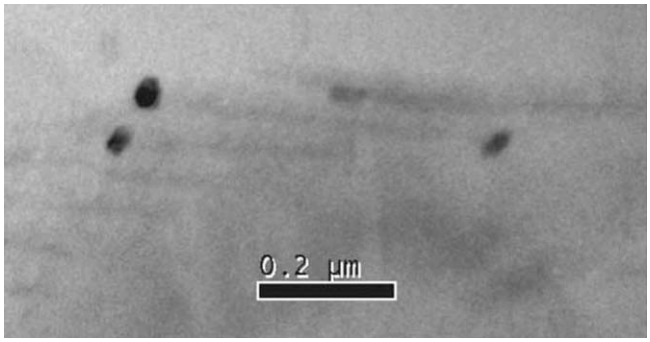

Fig. 3(a). Particles in alloy #2 (0.2 wt%Nb and 24 wt ppm Fe) annealed at 575 °C for 350 h.

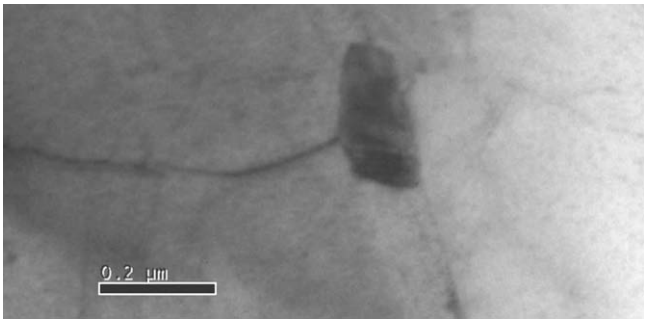

Fig. 4(a). Zr/Si/Fe/Ni/Cu particle in alloy #1 with 0.1 wt%Nb and <13 wt ppm Fe. Sample was annealed at 580 °C for 99 h.

consistent with a body-centred-cubic (bcc) crystal structure with a lattice parameter of ≈0.33 nm. Such precipitates have a high Nb content, ≈90 wt%Nb.

Small precipitates containing both Nb and Fe were observed in alloy #2 (0.2 wt%Nb), shown in Fig. 3(a), but there were no observations of β-Nb precipitates. The EDX spectrum of these precipitates is compared to the adjacent matrix in Fig. 3(b), showing the presence of NbK and FeK peaks that are associated with the

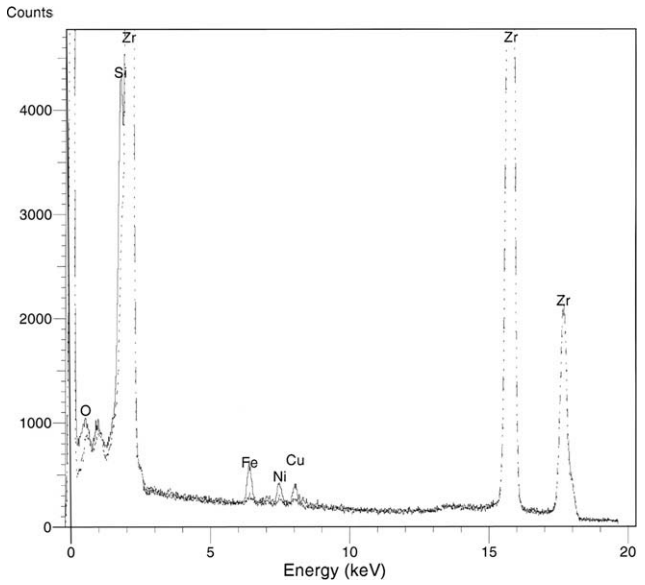

Fig. 4(b). EDX spectrum of a Zr/Si/Fe/Ni/Cu particle in alloy #1 that has 0.1 wt%Nb and <13 wt ppm Fe, compared to that of the α-Zr grain, showing Si, Fe, Ni and Cu peaks from the particle above those from the matrix. Top trace (solid line) is from the particle, while the bottom trace (dashed line) is from the α-Zr matrix. Sample was annealed at 580 °C for 99 h.

precipitates (solid lines) compared with the matrix (dotted lines). Figs. 3(a) and (b) also illustrates that some of the analyzed particles contained W or Si, or both. The particle density in alloys #2 and #3 was very low, on average one particle for roughly every 1 μm^2 in foil area.

Particles were also observed in TEM foils made from alloy #1 containing 0.1 wt%Nb and <13 wt ppm Fe. These particles contained Fe and Si, but no Nb. Fig. 4(a) shows a Zr/Si/Fe/Ni particle in this alloy that was annealed at 580 °C for 99 h; a corresponding EDX spectrum is shown in Fig. 4(b).

4. Discussion

This paper summarizes the results from observations of second phase particles in Zr–Nb alloys with Nb contents ranging from 0.10 to 0.86 wt% and low Fe content (<50 wt ppm) or higher Fe content, up to 470 wt ppm. The results show that impurities (Fe in particular) combine with Nb to form precipitates at Nb concentrations as low as 0.2 wt%. As these precipitates form at very low Fe concentrations it is very difficult to determine the Nb solubility in a pure Zr–Nb binary alloy. Thus if one assumes that once the Fe has formed precipitates, the remaining Nb in solution is somewhat representative of the solubility of Nb in α-Zr. An upper value for the limit of the solubility of Nb in α-Zr can then be defined.

Determination of the stoichiometry of the particles in alloys #2 and #3 would be extremely difficult because of their small size (<20 nm) and is beyond the scope of this work. Because the Fe removes Nb from solid solution, the concentration of Nb corresponding to the state where there is no beta-Nb is not known accurately. However the particle density in alloy #3 is estimated to be $<1 \times 10^{-19}$ per m^3, even if one assumes that the Nb content of the particles is 100% as an upper limit, then this corresponds to a reduction in Nb concentration in solid solution <0.001 wt%, i.e. well below the quoted accuracy of the Nb analysis for these alloys. One can therefore postulate that the solubility limit for Nb in a true binary alloy would be between 0.29 wt% and 0.49 wt%. This is contrary to the conclusions of [6].

The results also show that one cannot use the observation of particles as a criterion for establishing the solubility limit of Nb in the Zr–Nb binary system, because the results are always confounded by the effect of minor impurities, Fe in particular.

Acknowledgement

The experimental assistance of Michael Stewart is greatly appreciated.

References

[1] V.F. Urbanic, R.W. Gilbert, in: Proceedings of a Technical Committee Meeting organized by the International Atomic Energy Agency, Portland, Oregon, September 1989, IWGFPT-34, p. 262.
[2] V.F. Urbanic, M. Griffiths, in: D.S. Gelles, R.K. Nanstad, A.S. Kumar, E.A. Little (Eds.), Effects of Radiation on Materials: 17th International Symposium, ASTM STP 1270, American Society for Testing and Materials, Philadelphia, PA, 1996, p. 1088.
[3] V.F. Urbanic, M. Griffiths, in: G.P. Sabol, G.D. Moan (Eds.), Zirconium in the Nuclear Industry: 12th International Symposium, ASTM STP 1354, American Society for Testing and Materials, West Conshohocken, PA, 2000, p. 641.
[4] O.T. Woo, G.M. McDougall, R.M. Hutcheon, V.F. Urbanic, M. Griffiths, C.E. Coleman, in: G.P. Sabol, G.D. Moan (Eds.), Zirconium in the Nuclear Industry: 12th International Symposium, ASTM STP 1354, American Society for Testing and Materials, West Conshohocken, PA, 2000, p. 709.
[5] Y.H. Jeong, H.G. Kim, D.J. Kim, B.K. Choi, J.H. Kim, J. Nucl. Mater. 323 (2003) 72.
[6] H.G. Kim, J.Y. Park, Y.H. Jeong, J. Nucl. Mater. 347 (2005) 140.
[7] D.O. Northwood, D.C. Gillies, Microstruct. Sci. vol. 7 (1979) 123.
[8] I.T. Bethune, C.D. Williams, J. Nucl. Mater. 29 (1969) 129.
[9] O.T. Woo, G.J.C. Carpenter, in: Proceedings of the XIIth International Congress for Electron Microscopy, vol. 2, San Francisco, 1990, p. 132.
[10] C. Toffolon, J.C. Brachet, C. Servant, L. Legras, D. Charquet, P. Barberis, J.P. Mardon, in: G.D. Moan, P. Rudling (Eds.), Zirconium in the Nuclear Industry, 13th International Symposium, ASTM STP 1423, ASTM International, West Conshohocken, PA, 2002, p. 361.